energies

MDPI

Review

A Review of the External and Internal Residual Exhaust Gas in the Internal Combustion Engine

Nguyen Xuan Khoa [1] and Ocktaeck Lim [2,*]

[1] Faculty of Automobile Technology, HaNoi University of Industry, No. 298, Cau Dien Street, Bac Tu Liem District, Hanoi 100000, Vietnam; khoanx@haui.edu.vn
[2] School of Mechanical Engineering, University of Ulsan, 93 Daehak-ro, Nam-gu, Ulsan 44610, Korea
* Correspondence: otlim@ulsan.ac.kr

Abstract: Efficiency and emission reduction are the primary targets of internal combustion engine research due the large number of vehicles in operation and the impact of emissions-related pollution on human and ecosystem health. Harmful components of engine exhaust gases include nitrous oxides (NO_x), carbon dioxide, hydrocarbons, and particulate matter. NO_x emissions in particular are associated with significant health threats. The recirculation of exhaust gases can reduce NO_x emissions and improve engine efficiency when combined with other advanced techniques. On the other hand, the residual exhaust gas also effects on the quality of lubricating engine oil and therefore causes an increase in engine piston ring wear. In this review paper, the effects of external and internal exhaust gas recirculation on the performance and emission characteristics of diesel, gasoline, and alternative fuel engines are summarized and discussed in detail. Because it is difficult to estimate the internal residual exhaust gas in the combustion engine by doing experiments. This review paper introduces control strategies and prediction methods for internal and external exhaust gas recirculation.

Keywords: external exhaust gas recirculation; internal exhaust gas recirculation; NO_x emission; engine performance

check for updates

Citation: Khoa, N.X.; Lim, O. A Review of the External and Internal Residual Exhaust Gas in the Internal Combustion Engine. *Energies* **2022**, *15*, 1208. https://doi.org/10.3390/en15031208

Academic Editor: Andrzej Teodorczyk

Received: 14 December 2021
Accepted: 31 January 2022
Published: 7 February 2022

Publisher's Note: MDPI stays neutral with regard to jurisdictional claims in published maps and institutional affiliations.

Copyright: © 2022 by the authors. Licensee MDPI, Basel, Switzerland. This article is an open access article distributed under the terms and conditions of the Creative Commons Attribution (CC BY) license (https://creativecommons.org/licenses/by/4.0/).

1. Introduction

Several effective methods are available to improve internal combustion engine efficiency and reduce harmful emissions, including optimal ignition timing [1–3], optimal injection timing [4–6], alternative fuels [7,8], and turbocharger use [9,10].

The formation of nitrous oxides (NO_x) in the combustion chamber is strongly dependent on the peak firing temperature and oxygen concentration area [11,12]. Reducing either may help reduce NO_x emissions. Three methods are known to effectively reduce peak firing temperature and reduce NO_x emissions:

1. Using water injection [13–16]: Water is injected into the cylinder during the combustion stroke to reduce the temperature of the hottest area. This method may also help prevent engine knock [17].
2. Using a catalyst [18–20]: Engine exhaust gas flows through a catalyst before it is expelled to the environment. The catalyzers NH_3 and Mn-Ce/TiO_2 are known to reduce NO_x emissions.
3. Exhaust gas recirculation: A portion of an engine's exhaust gas recirculates back to the engine cylinders [21–24], resulting in a reduction in peak firing temperature and oxygen concentration area in the combustion chamber, which in turn reduces NO_x emissions.

Exhaust gas recirculation, which is discussed here in detail, can be classified into external exhaust gas recirculation (*eEGR*) [25,26] and internal exhaust gas recirculation (*iEGR*) [27–29].

In *iEGR*, the residual exhaust gases flow back into the combustion chamber through exhaust ports after each exhaust stroke. Premixing recirculated exhaust gases with a mixture of fresh air and fuel can affect combustion stability, charge mass, flame speed, and creation of toxic products in the next combustion stroke. This flow can be controlled by changing the intake valve timing, exhaust valve timing, and valve overlap period [30,31].

In *eEGR*, the gas from the exhaust pipe is routed back to the cylinder through the intake pipe. This is a useful and more effective method of reducing NO_x emissions in diesel engines [32–34] because up to 50% of the exhaust gases can be recirculated without affecting combustion stability. However, in gasoline engines, the *eEGR* rate should be kept below 20% to ensure combustion stability [35].

In a review of the effects of *eEGR* on the performance and emission characteristics of internal combustion engines, Abd-Alla [36] found that the *eEGR* method is more effective and provides greater benefits in terms of reducing NO_x emissions in diesel engine compared with gasoline and dual-fuel engines. In a gasoline engine, NO_x emissions can be reduced by 10% to 20%, but *eEGR* will also affect the combustion rate and reduce combustion stability. Greater *eEGR* reduces brake-specific fuel consumption (BSFC). For a dual-fuel engine, engine thermal efficiency can be improved with hot *eEGR* because a higher intake temperature allows for reburning of unburned fuel in exhaust gases. With cooler *eEGR*, the improvement in thermal efficiency is lower, but the reduction in NO_x emissions is greater.

Zheng et al. [37] reviewed the advances and novel concepts associated with *eEGR* in diesel engines, reporting that NO_x can be reduced, but particulate matter (PM) will increase because of lower oxygen concentrations. They identified several parameters that can influence *eEGR*, such as the pressure of the *eEGR* loop system, efficiency of the *eEGR* cooler, engine combustion efficiency, and temperatures of the intake and exhaust pipes. From those parameters, three methods of increasing *eEGR* efficiency were proposed. If *eEGR* gases are treated before returning to the cylinder, a greater reduction in NO_x emissions may be possible compared with using raw *eEGR*. The three methods of limiting *eEGR* are:

- *eEGR* cooling: the flow is cooled to reduce exhaust gas temperatures before returning to the cylinder.
- *eEGR* oxidation: The *eEGR* gases flow through a catalyst that oxidizes unburned combustibles into CO_2 and H_2O. This process extends the limits of *eEGR*.
- *eEGR* fuel reforming: an *eEGR* reformer produces H_2 and CO, increasing the premixed combustion rate.

In a review of the effects of *eEGR* on combustion ignition (CI) engine performance and emission characteristics, Harilal et al. [38] found that the *eEGR* method could be applied to CI engines with various fuels, including diesel oil, liquefied petroleum gas, bio-diesel, and hydrogen. At a 15% *eEGR* rate, fewer NO_x emissions were produced without a decrease in engine efficiency or BSFC.

Thangaraja et al. [39], who reviewed the effect of *eEGR* on advanced diesel combustion and alternative fuels, found that, while *eEGR* can reduce NO_x emissions, it also led to increased emissions of soot, particulate matter (PM), hydrocarbons, and carbon dioxide (CO). The increase in soot and PM can reduce the quality of engine lubrication oil, which increases engine wear.

A review of published articles confirmed that significant effects are associated with a reduction in NO_x emissions from exhaust gas recirculation. Most previous reviews and research articles focused on the effects of *eEGR* on CI engine performance and emission characteristics. No reviews discussed the effects of *iEGR* on engine performance and emission characteristics, which is a significant research gap. In this review paper, the effects of both *eEGR* and *iEGR* on internal combustion engines are highlighted, and the engine parameters or methods used to control or determine *eEGR* and *iEGR* will be discussed in detail.

2. External Exhaust Gas Recirculation

2.1. Effect of eEGR on Diesel Engine Performance and Emission Characteristics

The diesel engine offers relatively high fuel efficiency because it works at high compression ratios while experiencing little engine knock [40,41] compared with gasoline engines. However, these advantages come at the cost of greater NO_x and PM emissions and smoke [42]. Many strategies have been presented to control and reduce the harmful components of diesel emissions [43–45]. This section discusses in detail the effect *eEGR* on diesel engine performance and emissions.

Figure 1 provides a brief summary of the effects of *eEGR* on diesel engine performance and emission characteristics.

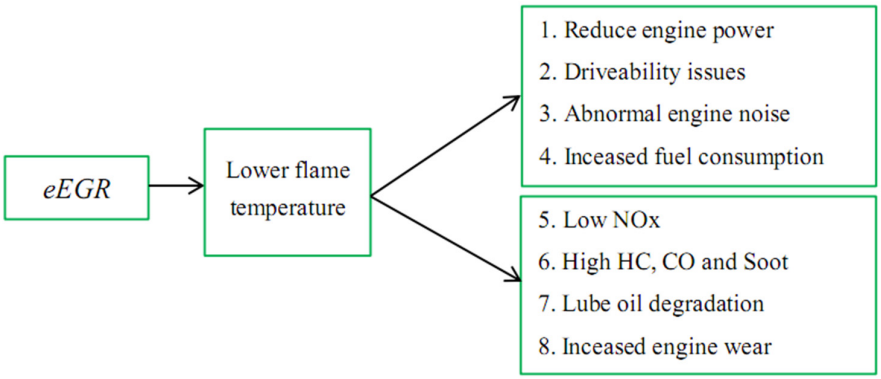

Figure 1. The effects of *eEGR* on diesel engine performance and emission characteristics.

An increase in the *eEGR* rate can dilute the intake of air into the combustion chamber. At a high temperature, *eEGR* increases the heat capacity of the intake charge and the endothermic dissociation of CO_2 and H_2O. This explains why an increase in the *eEGR* rate leads to a decrease in combustion quality and peak firing temperature. A decrease in NO_x emissions but lower engine power, high levels of hydrocarbons, CO, and soot are observed as a consequence. A higher soot level will negate the effect of lubricating oil additives and increase engine wear.

Torregrosa et al. [46] used a direct injection diesel engine to study the effects of *eEGR* on heat transfer in the combustion chamber. They found that *eEGR* has a large effect on heat transfer, with an increase in *eEGR* reducing combustion wall temperatures and cylinder heat flux. The greatest influence on heat flux was observed at the center of the cylinder head. A reduction in temperatures was associated with an *eEGR* rate of 18% to 30%.

Torregrosa et al. also found that the rate of decrease in percentage of NO_x emissions with *eEGR* was 10 times larger than the increase in percentage of CO_2 emissions.

An effect on carbon deposits and engine wear in an agricultural diesel engine at a constant engine speed is reportedly associated with *eEGR* [47]. The effect of *eEGR* rates of 0% to 20% on engine performance and emission characteristics at different engine loads was investigated. Figure 2 shows the relationship between the *eEGR* rate and engine thermal efficiency and NO_x emissions at different engine loads.

With an increase in the *eEGR* rate, engine thermal efficiency tends to increase slightly at lower loads because the unburned hydrocarbons from the previous cycle will be reburned. However, at high loads, *eEGR* rates of up to 20% result in little change in engine thermal efficiency because higher CO_2 levels reduce the peak firing temperature and oxygen concentration, and the unburned hydrocarbons from the previous cycle are therefore less significant. The decrease in peak firing temperature and oxygen concentration can also explain the sensitivity of NO_x reductions to high loads compared with low loads. Carbon deposits are more evident in engines using *eEGR* than those not using *eEGR* because of the greater soot emissions associated with engines using *eEGR*.

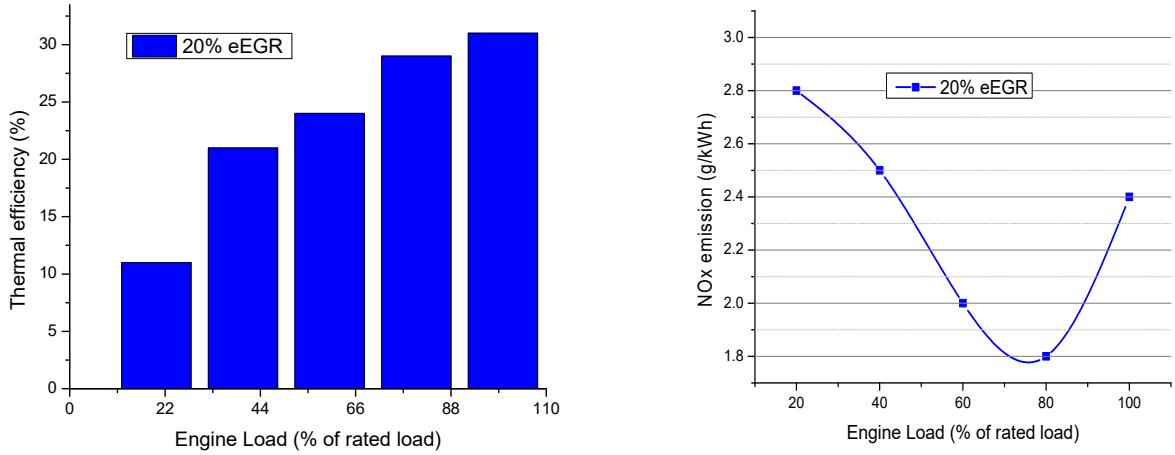

(**a**) (**b**)

Figure 2. Effect of 20% *eEGR* rate on: (**a**) engine thermal efficiency at difference engine loads; (**b**) NO_x emission at difference engine loads.

Table 1 shows a comparison between piston ring wear in engines using *eEGR* and those not using *eEGR*. In the case of piston ring number one, higher wear can be observed with engines not using *eEGR* because this piston ring experiences higher temperatures and pressures compared with rings in an engine using *eEGR*. With other piston rings, a reverse trend was evident because high soot emission in engines using *eEGR* reduces the quality of lubricating engine oil [48], the increase in *eEGR* leads to increased soot, which increases the friction between the piston ring and cylinder surface [49]. This also explains a higher wear of the other piston rings with *eEGR*.

Table 1. Effect of *eEGR* on piston ring wear.

Piston Ring Order	% Weight Loss	
	With *eEGR*	**Without *eEGR***
1	0.35	0.45
2	0.62	0.3
3	0.8	0.35
Oil ring	0.9	0.5

The effects of low- and high-pressure *eEGR* on the performance and emission characteristics of a turbocharged marine diesel engine at a low speed have also been examined [50]. Figure 3 shows the effects of high pressure *eEGR* on NO_x emissions at various engine loads and *eEGR* rates: a downward trend in NO_x emission at partial loads when the *eEGR* rate increased at both high and low pressures. With a higher *eEGR* rate, high-pressure *eEGR* was more effective in reducing NO_x emissions than low-pressure *eEGR*, although a higher BSFC was evident.

In summary, the benefits of using *eEGR* for a diesel engine include a reduction in NO_x emissions due to low combustion temperatures and cylinder head flux. In addition, improved thermal efficiency at low loads is possible with *eEGR*. However, *eEGR* will increase hydrocarbon, CO, and soot emissions; an increase in soot emissions will lead to increased carbon deposits, which reduces the quality of lubricating oil, causing increase engine wear.

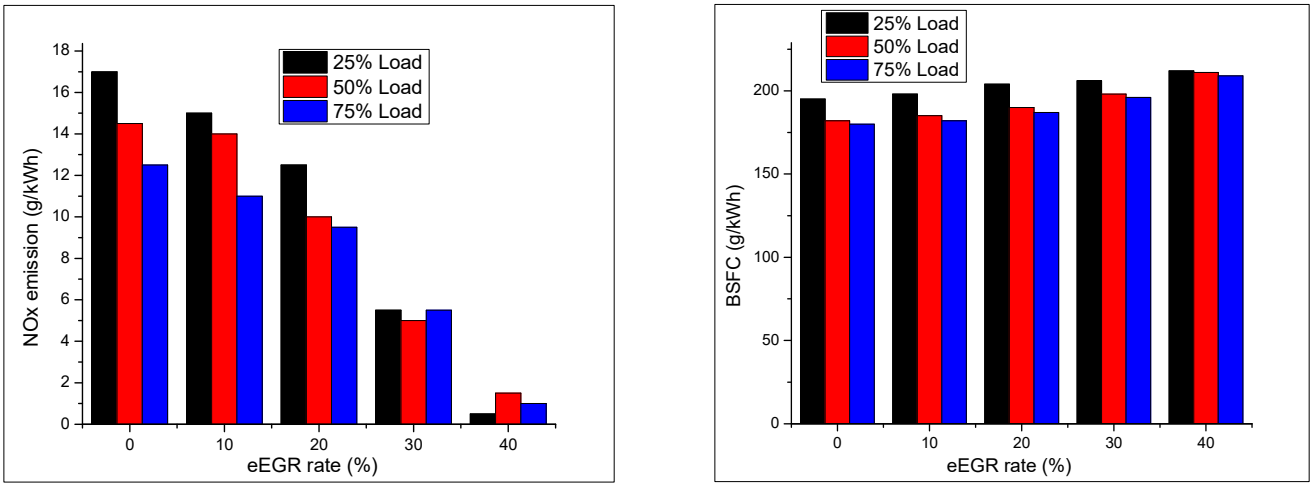

(**a**) (**b**)

Figure 3. Effect of: (**a**) high-pressure *eEGR* on NO_x emission; (**b**) high-pressure *eEGR* on BSFC.

2.2. Effect of eEGR on Alternative Fuel Engine Performance and Emission Characteristics

Alternative fuels offer a promising solution to fossil fuel security problems, the threat posed by greenhouse gas emissions responsible for climate change, and the health risks associated with the harmful components of exhaust gas. In addition, alternative fuels have become common and preferred racing fuels in recent years [51–57]. This section reviews the performance and emission characteristics of alternative fuel engines that use *eEGR*.

Yaopeng et al. [58] evaluated the influence of *eEGR* on the performance and emission characteristics of a compression ignition engine using methanol/diesel at medium loads. A three-dimensional simulation model based on the KIVA-3V code was employed to estimate the reductions in engine emissions and improvement in performance using *eEGR*. From the simulation results, they found that fuel efficiency improved with a higher methanol fraction and a low *eEGR* rate. Engine performance declined with an increasing *eEGR* rate, but a sharp reduction in NO_x emissions was also evident. A similar investigation of the effects of *eEGR* on engine emissions and combustion characteristics of an engine using ethanol was conducted by Saravanan et al. [59]. Their results also indicated that the peak firing temperature and exhaust gas temperature decreased due to a lack of oxygen in the combustion chamber at higher *eEGR* rates. The decrease in peak firing temperature and lack of oxygen was associated with a reduction in NO_x emissions and an increase in CO and hydrocarbon emissions.

Chunhua et al. [60] investigated the effect of *eEGR* on the combustion and emission characteristics of a six-cylinder dimethyl biodiesel-fueled engine. The experiments were conducted with biodiesel blends from 0% to 20% at both low loads (brake mean effective pressure (BMEP) = 0.4 MPa) and high loads (BMEP = 0.8 MPa). They reported that the ignition delay increased with the *eEGR* rate because a higher *eEGR* rate extended the interaction time between oxygen and fuel. A higher ignition delay at high loads compared with low load conditions can be observed in Figure 4. The increase in eEGR rate from 0% to 18% was due to a decrease in the flame-kernel growth rate from 16.5 m/s to 5.5 m/s, which was a product of an increase in eEGR, which reduced the spread of the ignition spark and flame velocity [61]. These results indicate that a hydrogen-fueled engine can operate without knock at a higher equivalence ratio by applying eEGR.

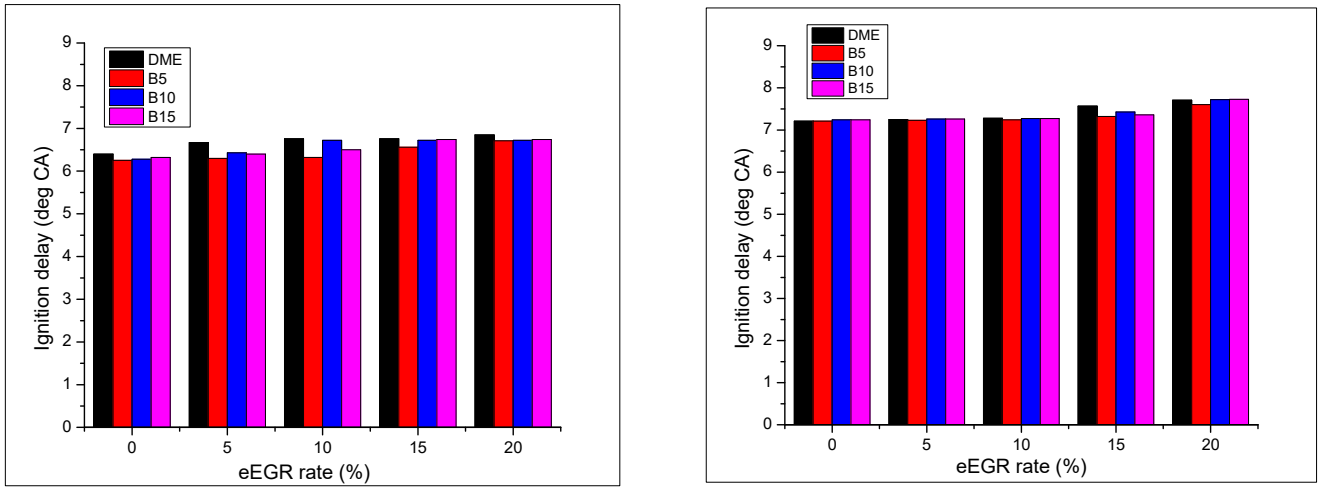

(**a**) (**b**)

Figure 4. Effect of *eEGR* rate on ignition delay at: (**a**) low load (BMEP = 0.4 MPa); (**b**) high load (BMEP = 0.8 MPa).

An increase in the *eEGR* rate can reduce the flow of fresh air into a cylinder, leading to a reduction in oxygen and homogeneous air–fuel for the combustion process. As a result, both the combustion phase and duration tend to increase with a higher *eEGR*, and this effect is enhanced at high loads (Figure 5).

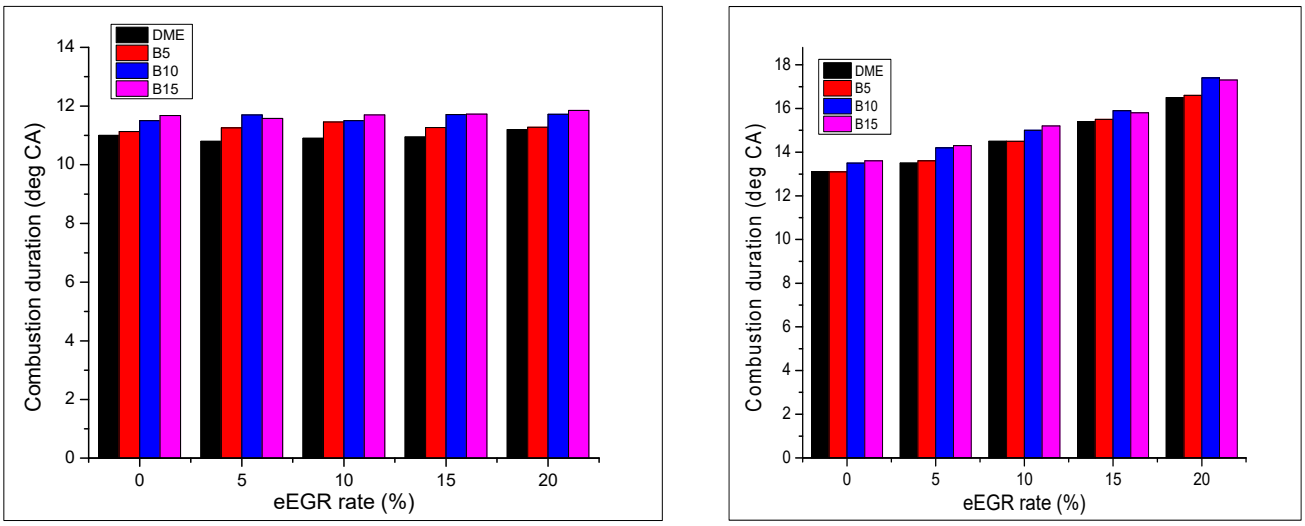

(**a**) (**b**)

Figure 5. Effect of *eEGR* rate on combustion duration at: (**a**) low load (BMEP = 0.4 MPa); (**b**) high load (BMEP = 0.8 MPa).

A lack of O_2 and reduced homogeneous air–fuel mixture decreases the heat release rate and pressure rise. A lagging peak heat release rate and peak pressure rise with an increase in the *eEGR* rate.

In these results, a significant effect from the increased *eEGR* rate was observed in the form of reduced NO_x emissions but increased hydrocarbon and CO emissions, as in a diesel engine.

Salvi et al. [62,63] conducted an experiment and simulations using a single-cylinder, spark-ignition engine with hydrogen as a fuel to study the effect of *eEGR* on the flame kernel

growth rate. The experiment was conducted at an engine speed of 3000 rpm; hydrogen was injected through an intake manifold by a gas injector, and the *eEGR* rate varied from 0% to 18% by volume. Figure 6 shows that the increase in the *eEGR* rate from 0% to 18% was due to a decrease in the flame kernel growth rate from 16.5 m/s to 5.5 m/s, which was a product of an increase in *eEGR*, which reduced the spread of the ignition spark and flame velocity [64]. These results indicate that a hydrogen-fueled engine can operate without knock at a higher equivalence ratio by applying *eEGR*.

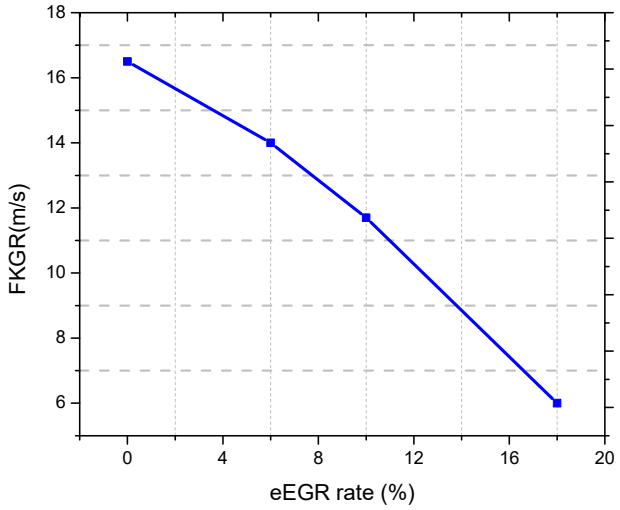

Figure 6. Effect of *eEGR* rate on the flame kernel growth rate.

Yasin et al. [65] studied the performance of an engine fueled by palm oil biodiesel, combining an experiment with simulations to estimate the effect of *eEGR* at full loads and an engine speed of 2000 rpm. They found BSFC and CO emissions increased while exhaust gas temperature and NO_x emissions decreased when using *eEGR* compared with the same engine fueled by diesel (Figures 7 and 8). The lower heat value of biodiesel fuels means the peak firing temperature and exhaust gas temperature will be lower compared with conventional diesel fuel. As a result, lower NO_x emissions and higher CO emissions were reported using biodiesel fuel with *eEGR*.

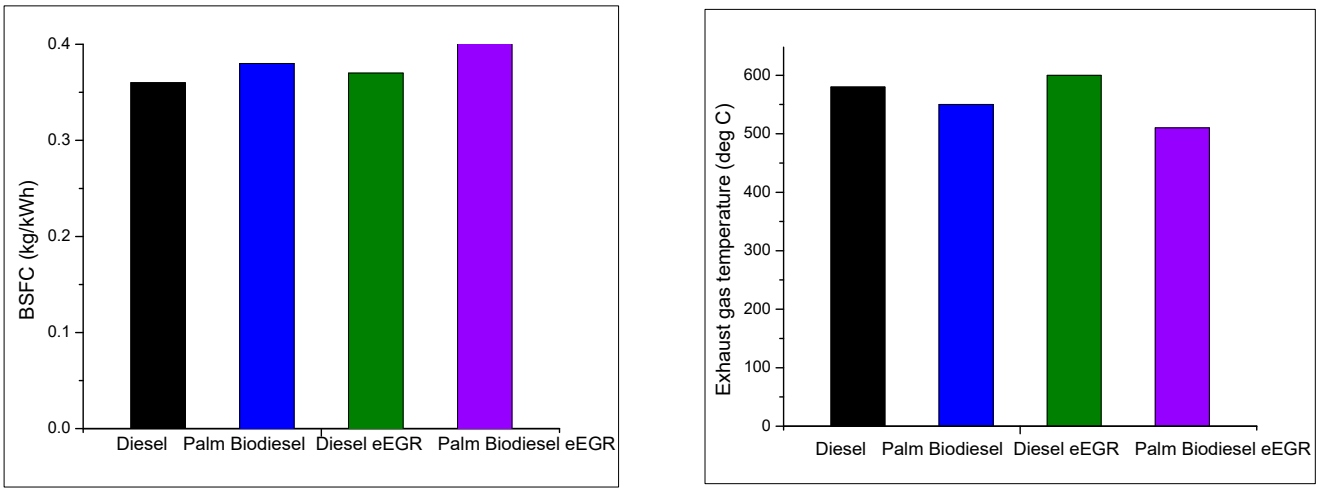

Figure 7. A comparison of the effect of *eEGR* rate on BSFC and exhaust gas temperature between diesel and palm oil biodiesel.

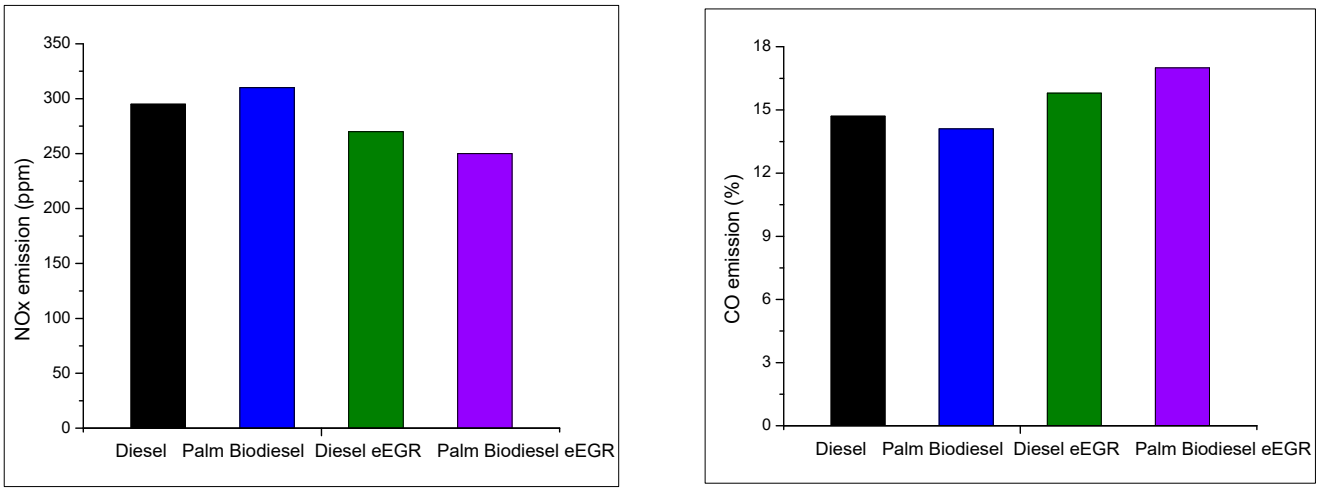

Figure 8. A comparison of the effect of *eEGR* rate on NO_x and CO emissions between diesel fuel and palm oil biodiesel [65].

In summary, in an engine using an alternative fuel, a downward trend in NOx emissions and an upward trend in hydrocarbon and CO emissions was associated with an increased *eEGR* rate. The increased *eEGR* led to an increase in ignition delay, combustion phase, and combustion duration because the dilution charge extended the interaction time between oxygen and the fuel. A hydrogen-fueled engine can therefore be operated without knock at a higher equivalence ratio by applying *eEGR*.

2.3. Effect of eEGR on Spark Ignition Engine Performance and Emission Characteristics

Among different approaches to improving engine performance, *eEGR* is a promising approach to suppressing knock, improving engine efficiency, and reducing NO_x emissions in spark ignition engines [66–68]. This section provides a review of the effect of *eEGR* on spark ignition engines.

Thomas et al. [69] studied the suppression of knock in a direct injection spark ignition engine using *eEGR*. The *eEGR* rate was increased from 0% to 13% at three load conditions of the indicated mean effective pressure (IMEP: 5.5 bar, 7.0 bar, and 8.5 bar). They reported that an increased *eEGR* helped reduce the indicated specific fuel consumption (ISFC) by 2.2%, 4.1%, and 1.0%, respectively. At 7.0 bar (the IMEP test case), the engine achieved a knock-limited maximum torque at 8 deg-CA with a 12% *eEGR*, which led to improved peak cylinder pressure, ISFC, and engine efficiency; the pumping work was reduced at the knock-limited maximum brake torque, and the engine achieved optimum engine load phasing. The ISFC could be further improved if the *eEGR* incorporated a three-way catalyst [70]. The decrease in NO_x emissions and increase in hydrocarbon emissions were linked to a decrease in peak firing temperature as the *eEGR* increased.

Dongwon et al. [66], who investigated the potential of *eEGR* to improve the thermal efficiency and emission characteristics of a spark ignition engine, found that engine efficiency could be improved by 16% with *eEGR*, lean combustion, and a fuel–air equivalence ratio of 0.7. Other research teams have reported that a similar degree of maximum thermal efficiency could be obtained with a combination of *eEGR* and lean burning conditions [71].

Atul et al. [72] reported the effect of exhaust *eEGR* on spark ignition engine performance and emission characteristics. Using a 2.0 L four-stroke engine, they increased the *eEGR* rate from 0% to 19%, reporting that the increase in *eEGR* rate was due to an increase in combustion duration because the charge dilution from incorporating *eEGR* decreased flame speed and propagation. The increase in *eEGR* reduced the amount of fresh air and oxygen in the combustion chamber, reducing the peak firing temperate and BMEP, as shown in Figure 9.

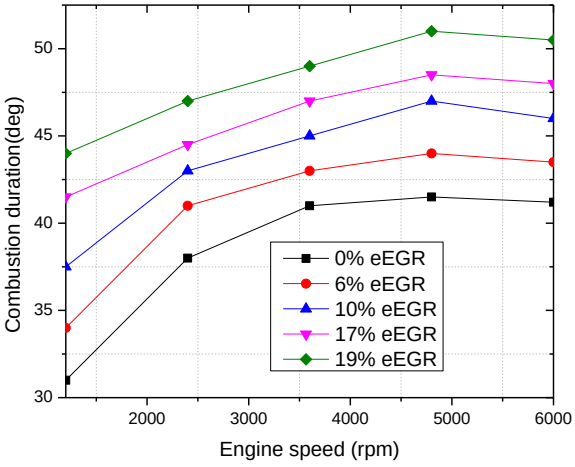

(**a**)

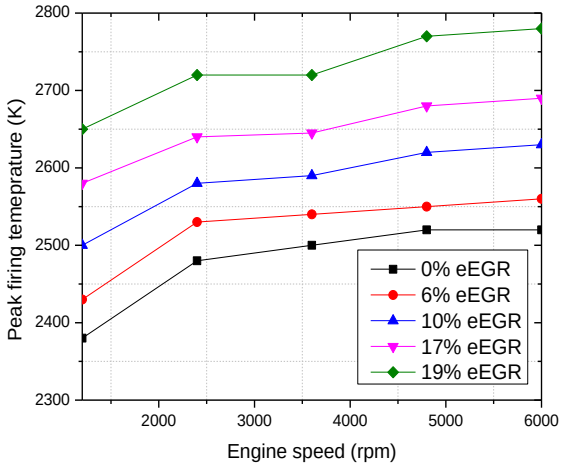

(**b**)

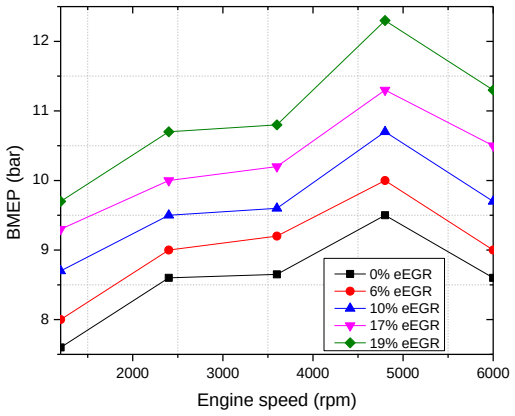

(**c**)

Figure 9. The effect of *eEGR* on: (**a**) combustion at various engine speeds; (**b**) peak temperature at various engine speeds; (**c**) BMEP and BSFC at various engine speeds.

A reduction of NO_x and CO emissions and increase in hydrocarbons is reported. These effects can be attributed to the decrease in peak firing temperature and amount of oxygen in the air during combustion. When the *eEGR* rate rose to 19%, the engine achieved a 20% decrease in BMEP, and NO_x and CO emissions fell from 20% to 33%. However, BSFC and hydrocarbon emissions increased by 2.5% and 50%, respectively. The ignition delay increased with the *eEGR* rate because a higher *eEGR* rate increased the charge dilution, which extended the interaction time between O_2 and fuel [73].

Currently, *eEGR* is commonly used in spark ignition gasoline engines because of its ability to increase engine efficiency, reduce NO_x emissions, and suppress knock, although the latter requires careful control techniques.

2.4. Control System and Prediction of eEGR Methods

In the *eEGR* method, the exhaust gas from an engine will be reburned by returning a part of exhaust gas to the intake tube and allowing it to mix with fresh air and fuel in the combustion chamber. Unburned hydrocarbons in the exhaust gas will be burned completely, and the resulting charge dilution can reduce peak firing temperature and oxygen concentrations, which reduces NO_x emissions. The *eEGR* rate can be controlled by a valve as shown in Figure 10.

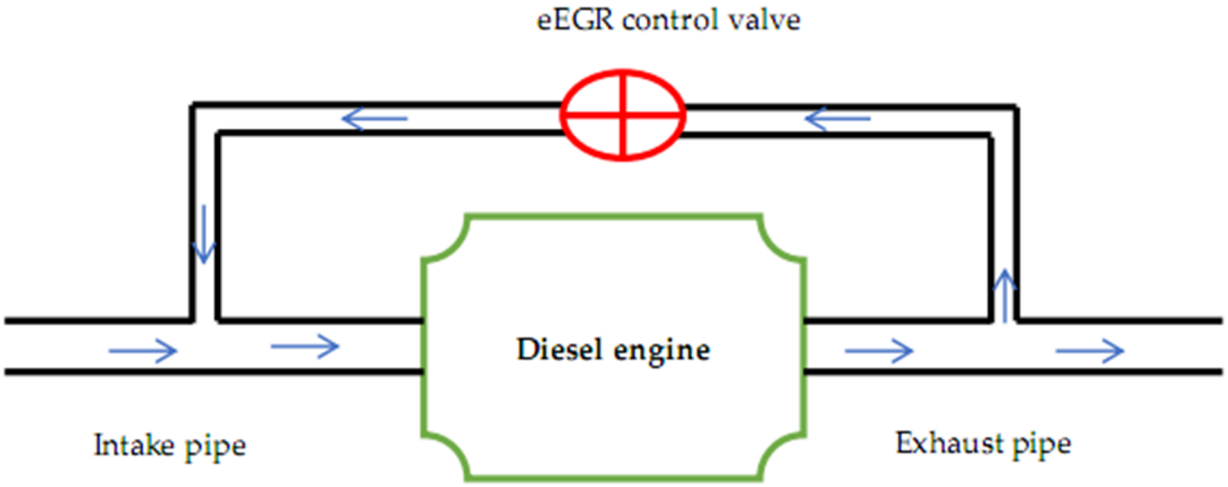

Figure 10. A simple *eEGR* loop system.

Figure 10 shows that the exhaust gas in an *eEGR* system returns directly to the intake pipe at a high temperature due to a reduction in engine volume efficiency and a high charge dilution. As this decreases engine efficiency and promotes knock, other effective designs of an *eEGR* loop system are required to eliminate these drawbacks, as shown in Figures 11 and 12.

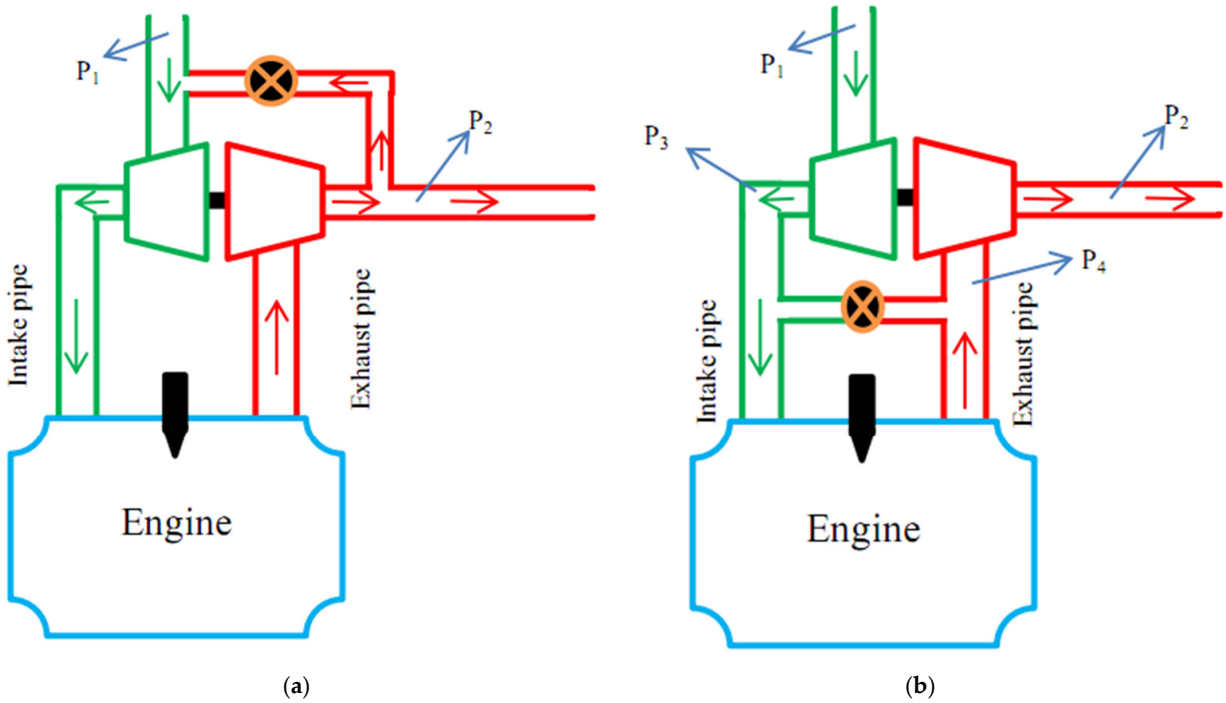

Figure 11. *eEGR* loop system: (**a**) Low-pressure *eEGR* flow; (**b**) high-pressure *eEGR* flow.

Figure 11 depicts two schemas for an *eEGR* loop system. The *eEGR* flow will reduce temperatures before returning the exhaust gases to an inlet pipe, improving volume efficiency and reducing knock [74]. Figure 11a describes an *eEGR* loop system with low-pressure *eEGR* flow through the turbine. Exhaust is directed to the intake pipe when P_2 is higher than P_1.

Figure 11b describes an *eEGR* loop system with high-pressure *eEGR* flow. The *eEGR* flow is directly charged to the intake pipe when P_4 is higher than P_3.

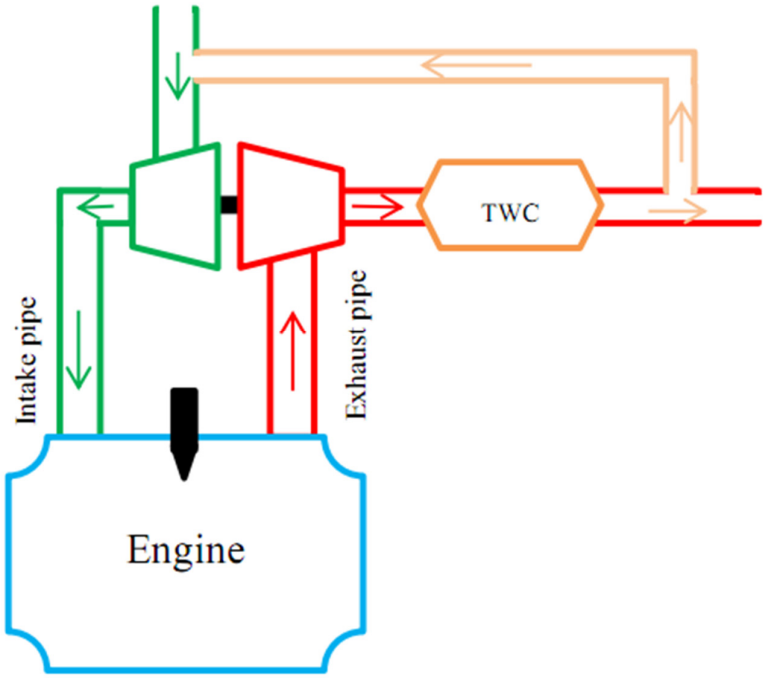

Figure 12. Clean *eEGR* circuits.

Figure 12 depicts an *eEGR* system that uses a three-way catalytic converter to reduce NO_x and PM before the exhaust gases reach the intake pipe.

Previous studies have used a set of equations to calculate the *eEGR* rate:

The high-pressure and cooled *eEGR* rate is defined from the mass flow rate [75]

$$eEGR\ \% = \frac{m_{eEGR}}{m_i} \cdot 100 \quad (1)$$

where m_{eEGR} is the *eEGR* mass, and m_i is total mas intake mixture.

The high-pressure and cooled *eEGR* rate is defined from the volume flow rate [75]

$$eEGR\ \% = \frac{V_{af} - V_{ac}}{V_{af}} \cdot 100 \quad (2)$$

where V_{af} is the air flow volume rate into the engine at full load without *eEGR*.

V_{ac} is the air flow volume rate into the engine at part load with *eEGR*.

The high-pressure and uncooled *eEGR* rate is defined from concentration of CO_2 [76]

$$eEGR\ \% = \frac{[CO_2]_{inlet} - [CO_2]_{ambient}}{[CO_2]_{exhaust} - [CO_2]_{ambient}} \quad (3)$$

where $[CO_2]_{inlet}$ is the concentration of CO_2 at inlet pipe.

$[CO_2]_{exhaust}$ is the concentration of CO_2 at exhaust pipe.

$[CO_2]_{ambient}$ is the concentration of CO_2 at ambient.

The low-pressure and cooled *eEGR* rate is defined from concentration of CO_2 [77]

$$eEGR\ \% = \frac{[CO_2]_{inlet} - [CO_2]_{ambient}}{[CO_2]_{exhaust}} \quad (4)$$

where $[CO_2]_{inlet}$ is the concentration of CO_2 at inlet pipe.

$[CO_2]_{exhaust}$ is the concentration of CO_2 at exhaust pipe.

The simulation *eEGR* rate is defined from the nitrogen mass [78]

$$eEGR\ \% = \frac{m_{N_2}}{m_{air} + m_{N_2}} \quad (5)$$

where m_{N_2} is the N_2 mass flow; m_{air} is the total charged air mass.

The simulated *eEGR* rate is determined by the inherent and applied residual gas ratios for a two-stroke engine [79]

$$eEGR\% = \left(\gamma_{ap} - \gamma_{inh}\right) \cdot 100\% \quad (6)$$

where γ_{ap} is the applied residual gas ratio; γ_{inh} is the inherent residual gas ratio.

Based on the experimental conditions and an *eEGR* loop system, a suitable *eEGR*-rate equation should be selected for optimal results.

3. Internal Exhaust Gas Recirculation (*iEGR*)

The *eEGR* flow is taken from the exhaust pipe and supplied to the cylinder through the inlet pipe, while *iEGR* is achieved by modifying the intake or exhaust valve profile to increase the fraction of exhaust residuals at the end of the intake stroke. This section discusses the effect of *iEGR* on engine performance and emission characteristics.

3.1. The Effect of iEGR on Engine Performance and Emission Characteristics

In an internal combustion engine, *iEGR* can reduce NO_x emissions, while intake and exhaust valve timing is used to control the reverse exhaust gas flow back into the cylinder.

A comparison of the effects of *eEGR* and *iEGR* on the performance and emission characteristics of a six-cylinder, four-stroke diesel engine was conducted via experiments and simulations [80]. A variable valve actuation system was used to control valve timing, which increased *eEGR* flow back into the cylinder. Using *iEGR* with the same exhaust gas recirculation rate and full load conditions resulted in lower NO_x emissions, lower engine torque, and higher BSFC compared with *eEGR*. This can be attributed to the higher temperature and pressure of the *iEGR* mass in the combustion chamber, which lowered the air–fuel mixture density and decreased engine volume efficiency, reducing oxygen concentration, peak firing temperature, and engine efficiency. However, when the engine operated in a transient state, *iEGR* was associated with superior control of the exhaust gas recirculation rate compared with *eEGR*.

The combustion characteristics of a homogeneous charge compression ignition engine using biogas as a fuel can be altered using *iEGR* [81]. An increase in the *iEGR* rate due to dilution of the oxygen in the air–fuel mixture causes an increase in combustion duration and timing and a lower increase in combustion duration with the *iEGR* band from 1.5% to 10% when compared with the *iEGR* band from 10% to 20% as a result.

The emission characteristics of a spark ignition engine using natural gas and ethanol as fuel can be controlled using *iEGR*. When the *iEGR* rate was increased from 9.5% to 14%, NO_x emissions decreased by 67%, but CO and hydrocarbon emissions increased by nearly 75% [82] as shown in Figure 13. An increase in ignition delay and combustion duration was also evident [83].

In a gasoline engine, the *iEGR* can be an effective method of improving efficiency and reducing NO_x emissions. Such engines can achieve stable combustion rates at low loads with *iEGR* [84]. When the *iEGR* rate was increased from 9.1% to 51.7%, the BMEP increased after achieving a maximum value at an *iEGR* rate of 22.8%, after which the *iEGR* continued to increase. The BSFC exhibited a contrary trend to that of the BMEP; the optimal BSFC was achieved at 202 g/kWh, with an *iEGR* rate of 22.8%. This makes it clear, at low load conditions, the high temperature of a suitable *iEGR* rate helps engines achieve superior homogeneous air–fuel mixtures and combustion processes [85]. However, a high *eEGR* rate can cause charge dilution, increasing the incomplete combustion rate and low burning

conditions and decreasing thermal efficiency [86]. When an engine is idling, a high *iEGR* rate can effectively reduce cycle-to-cycle variation and improve combustion stability.

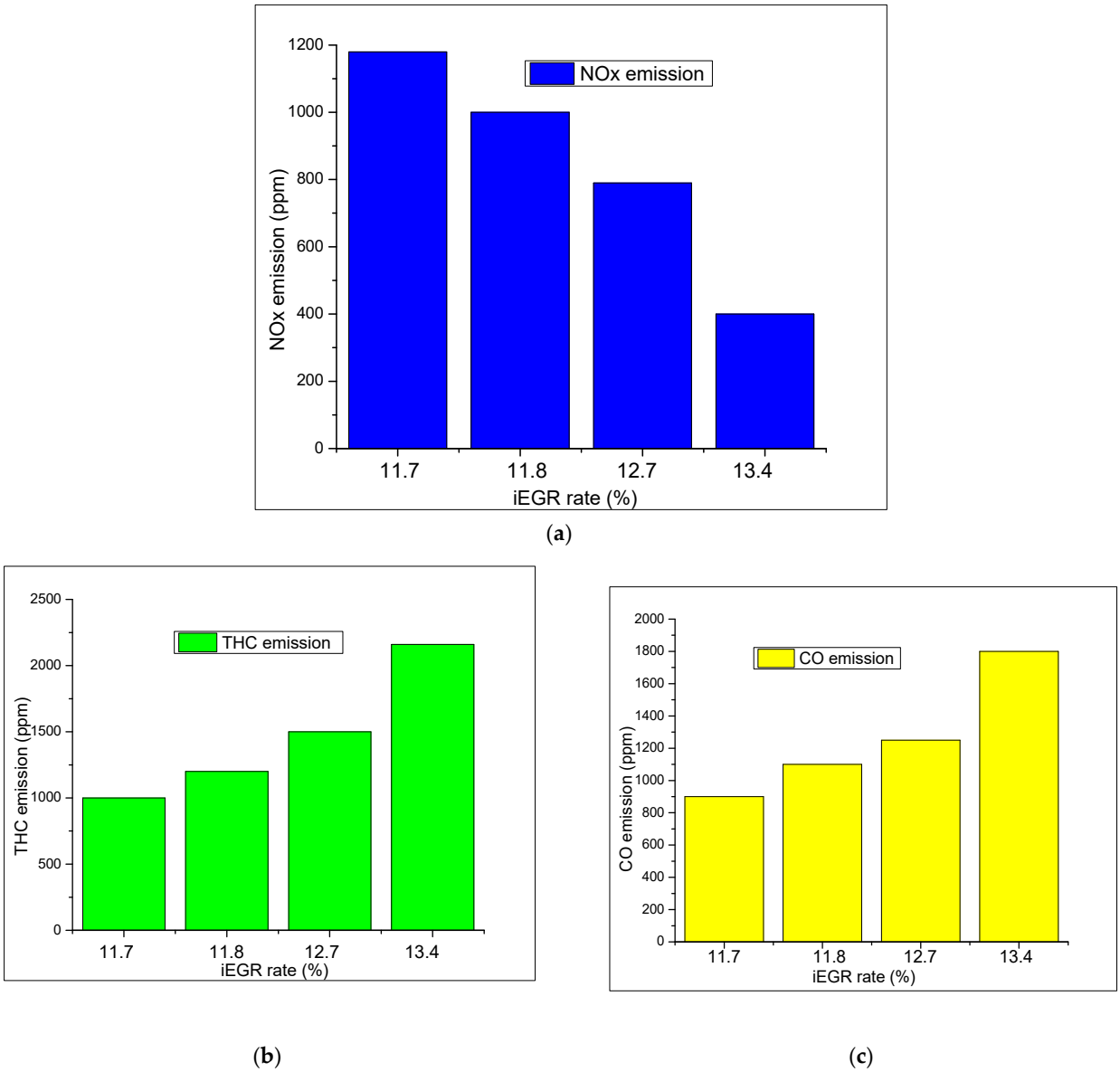

Figure 13. The effect of *iEGR* on: (**a**) NO_x; (**b**) THC; (**c**) CO emission.

The close relationship between combustion duration and *iEGR* in small spark ignition engines fueled by gasoline has been investigated [87]. In a further study, the effect of *iEGR* on engine performance and emission characteristics at full loads was investigated.

The *iEGR* rate has a significant effect on peak firing temperature and pressure rise [88]. Figure 14a,b shows decreases in peak firing temperature and pressure rise with an increasing *iEGR* rate. This is because the higher *iEGR* rate was due to a diluted and less homogeneous air–fuel mixture and a lack of oxygen. This led to a decrease in the quality of combustion and the heat release rate of the power stroke. The results of the research show that the peak firing temperature decreased from 2900 K to 1250 K, and the peak pressure rise decreased from 8 bar/deg to 5.5 bar/deg, respectively.

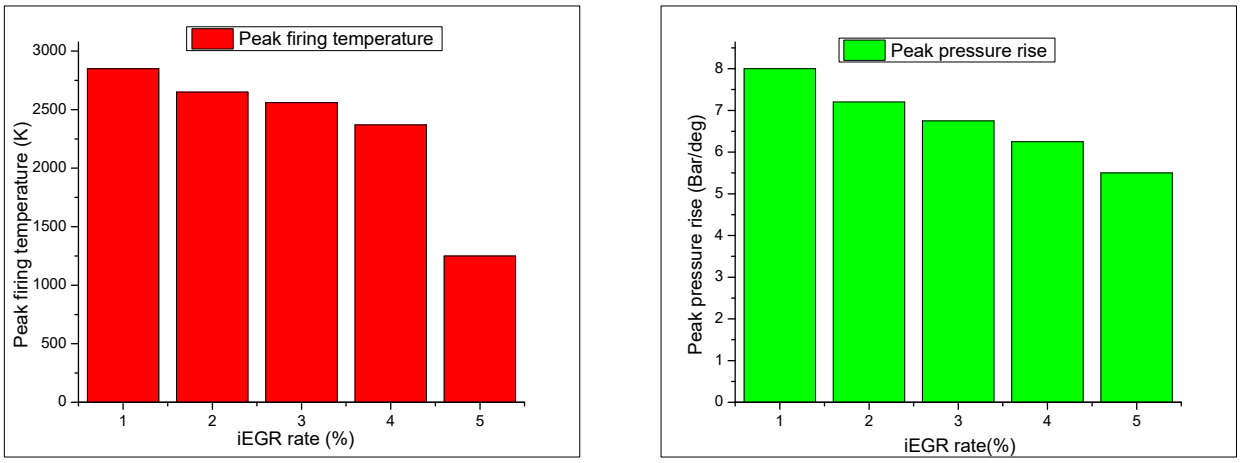

(**a**) (**b**)

Figure 14. The Effect of *iEGR* on: (**a**) Peak firing temperature; (**b**) peak firing pressure.

In a combustion stroke, the chemical energy trapped in the cylinder is released as heat. A certain amount of heat energy is lost through heat transfer, pumping loss, and energy that is not effectively released in the cylinder (but instead goes into the combustion products). The remaining energy is the effective release energy. A decrease in effective release energy (Figure 15a) with an increase in residual exhaust gas was observed. To increase thermal efficiency, a short burn time can lead to a faster release of heat energy. However, the increase in residual gas in the cylinder due to a longer burn time, lower peak firing pressure rise, and lower peak firing temperature reduces the effective release energy. The effective release energy decreased from 0.85 KJ to 0.53 KJ when the *iEGR* increased from 1% to 5%.

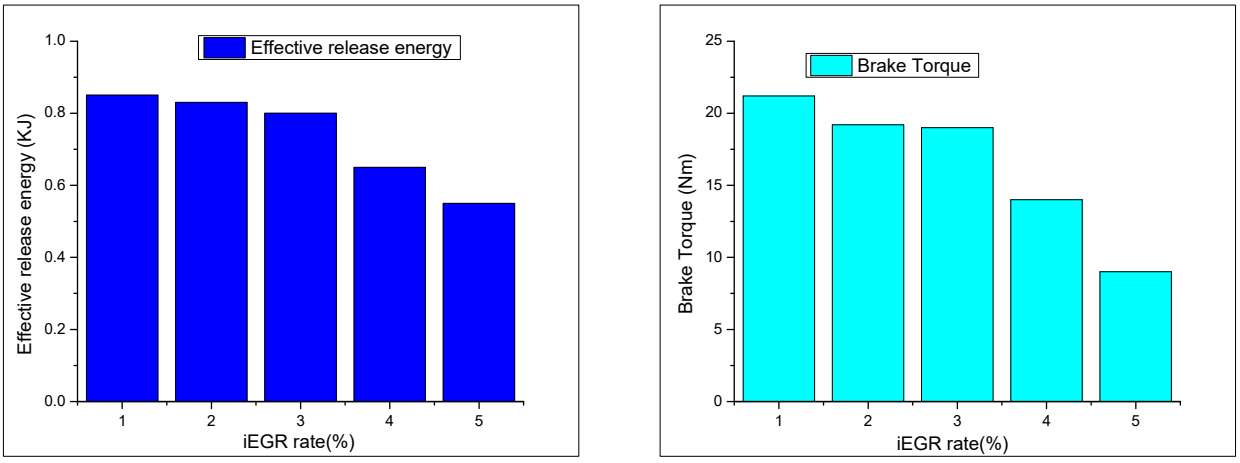

(**a**) (**b**)

Figure 15. The effect of *iEGR* on (**a**) Effective release energy; (**b**) brake torque.

The increase in *iEGR* led to a decrease in the heat release rate and effective release energy, so the decrease in engine torque is a result (Figure 15b).

Figure 16a shows that NO_x emissions tend to decrease with an increasing *iEGR* rate for two reasons. First, an increased *iEGR* is associated with a lower peak firing temperature. Second, an increase in *iEGR* is caused by a diluted air–fuel mixture and less oxygen. NO_x emissions declined to a minimum of 2.12 g/kWh at a residual gas ratio of 5%. Figures 16b,c show that an increased residual gas ratio leads to increased HC and CO emissions. This is

because the higher residual gas ratio leads to an increased diluted air–fuel mixture and an increase in the areas lacking oxygen, increasing the amounts of unburned hydrocarbons and CO emissions from 3.65 g/kwh to 18.2 g/kwh and 139 g/kwh to 450 g/kwh, respectively.

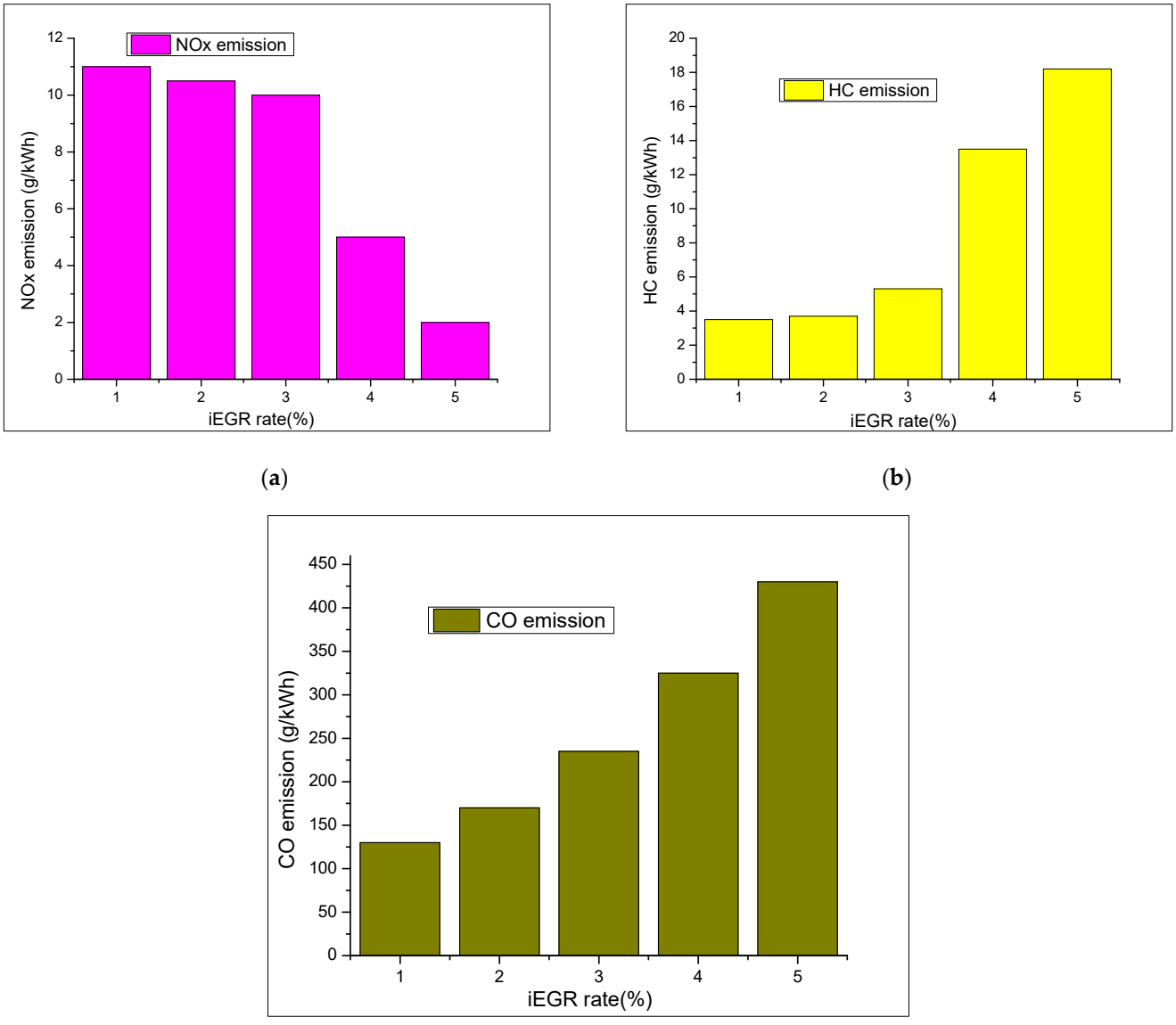

Figure 16. The effect of *iEGR* on egine emission versus *iEGR* [88]: (**a**) NOx emission; (**b**) HC emission; (**c**) CO emission.

In summary, *iEGR* and *eEGR* result in similar effects on engine performance and emission characteristics. Using *iEGR* has less of an effect on NO_x because the exhaust gas recirculation rate is lower than that of *eEGR*. However, *iEGR* involves a lower initial cost, simpler packaging, a potential for retrofit, lower maintenance costs, greater reliability, and higher tolerance of high-sulfur fuels. Using *iEGR* also offers improved cold engine starts and shorter warm-up periods.

3.2. Control Strategies and Prediction of iEGR Methods

Engine speed, load conditions, and valve overlap can effect *iEGR* performance [89]. To obtain a target *iEGR* mass at a steady state, controlling valve overlap has proven to be an effective approach. Valve overlap is the time during which both the inlet and exhaust

valves are both open, which permits *iEGR* flow to return to the cylinder. The timing of the intake opening and exhaust closing has a strong influence on valve overlap. In an internal combustion engine, intake valve timing controls the intake flow into the cylinder while the exhaust gas flow is controlled by exhaust valve timing. Early intake valve opening may cause exhaust gases to be expelled into the intake port and back to the cylinder in the intake stroke, and late exhaust valve opening may result in the reverse exhaust flow back to the cylinder during the intake stroke [90]. The *iEGR* rate can be controlled by changing the timing of the intake valve opening timing and the exhaust valve closing. The increase in the early opening of the intake valve or late closing of the exhaust valve can cause an increase in the *iEGR* rate.

The ability of a fully flexible variable valve actuation (FVVA) system without camshafts to provide a fully independent lift of intake and exhaust valves was recently tested. Such FVVA systems can be electrohydraulic [91,92], electropneumatic, or electromagnetic [93]. The FVVA system allows for a secondary lift of an intake valve during the exhaust stroke (2IVO) or induces a secondary lift of an exhaust valve during the intake stroke (2EVO) [94,95].

Benajes et al. [96] studied the effect of the 2IVO and 2EVO approaches on the *iEGR* rate of a heavy-duty diesel engine. The authors reported that the 2IVO strategy resulted in a higher *iEGR* rate than that of a 2EVO approach because the latter reduced air mass flow and disrupted swirl production. When applying the 2IVO strategy to an engine, an *iEGR* rate of up to 12% was achieved. Combining 2IVO and valve overlap strategies in a high-speed, direct injection engine resulted in an *iEGR* of up to 25% [97]. An *iEGR* of 60% was possible using a combination of 2IVO and 2EVO strategies [98]. Thompson et al. [99] investigated the effect of *iEGR* on the performance and emissions of a spark-ignition engine at partial loads, using FVVA to control the positive and negative valve overlaps to increase the *iEGR* from 5% to 35%. The engine achieved a combustion efficiency of 25% to 30%.

At each operating condition with a suitable *iEGR* rate, the engine will perform at optimal combustion efficiency. An accurate method to determine the *iEGR* rate is therefore necessary. It is difficult to determine *iEGR* by doing experiments, so the *iEGR* rate can be obtained from the inherent and applied residual gas ratio through the simulation method [79]

$$iEGR\% = \left(\gamma_{ap} - \gamma_{inh}\right) \cdot 100\% \tag{7}$$

where γ_{ap} is the applied residual gas ratio; γ_{inh} is the inherent residual gas ratio.

The total *iEGR* rate can be calculated based on the mass without *eEGR* [99–101]

$$iEGR\ \% = \frac{m_b}{m_m + m_b} \cdot 100\% \tag{8}$$

where m_b is the mass of simulated residual exhaust gas; m_m is the air–fuel mixture mass.

The simulated *iEGR* rate can be determined when the engine combines *iEGR* and *eEGR* [84]

$$iEGR\ \% = \frac{m_b}{m_m + m_{eEGR} + m_b} \cdot 100\% \tag{9}$$

where m_{eEGR} is the mass of external exhaust gas recirculation.

4. Conclusions

Through this review, the effect of internal and external exhaust gas recirculation was completely discussed, and the mentioned gap of internal exhaust gas recirculation reviews has been filled. Based on the review of *iEGR* and *eEGR*, the important results are summarized below:

- Due to the benefits of reducing NO_x emissions and improving ISFC and engine efficiency, both *iEGR* and *eEGR* are commonly used in modern internal combustion engines. Gasoline engines can improve ISFC and engine thermal efficiency at low loads, while hydrogen-fueled engines can operate without knock at a higher equivalence ratio.

Exhaust gas recirculation can be used to suppress knock, improve engine efficiency, and reduce NO_x emissions from a spark-ignition engine, but requires a high degree of precise technical control.

- Internal combustion engines using exhaust gas recirculation can reduce NO_x emissions due to the resulting decrease in combustion temperatures, cylinder head flux, and oxygen concentrations. However, exhaust gas recirculation will increase hydrocarbon, CO, and soot emissions, ignition delays, and combustion duration. The increase in soot emission is due to increased carbon deposits, which also reduce the quality of lubricating engine oil and therefore causes an increase in engine wear. The increase in combustion duration is due to increased heat loss transfer.
- The *iEGR* method reduces NO_x emissions to a lesser extent than the *eEGR* method because the exhaust gas recirculation rate is lower with *iEGR*. However, *iEGR* involves a lower initial cost, easier packaging and the potential for retrofits, lower maintenance cost, greater reliability, and a higher tolerance of high-sulfur fuels. It offers improved cold engine starts and warm-up periods.
- Exhaust gas recirculation control strategies, and determination equations for *eEGR* and *iEGR* were also reported. Depending on an engine's operating condition, a suitable combination of an exhaust gas recirculation control strategy and determination equation should be selected for optimal efficiency.

Author Contributions: Conceptualization, N.X.K.; methodology, N.X.K.; software, N.X.K.; validation, N.X.K.; resources, N.X.K.; O.L; writing—original draft preparation, N.X.K.; writing—review and editing, N.X.K., O.L; supervision, O.L.; project administration, O.L. All authors have read and agreed to the published version of the manuscript.

Funding: This research was funded by the individual basic research project by the National Research Foundation of Korea (NRF-2021R1F1A1048238, Reliability Improvement of Ammonia-Diesel Dual-Fuel Combustion Model regarding Optimized Combustion Strategy for Improved Combustion Efficiency and Emission Characteristics). This research is financially supported by the Shipbuilding and Offshore Industry Core Technology Development Business by the Ministry of Trade, Industry and Energy (MOTIE, Korea) [Develop-ment of Low Print Point Alternative Fuel Injection System for Small and Medium Vessel Engines for Ships Hazardous Emission Reduce]. (20013146).

Institutional Review Board Statement: Not applicable.

Informed Consent Statement: Not applicable.

Data Availability Statement: Not applicable.

Conflicts of Interest: The authors declare no conflict of interest.

References

1. Lim, G.; Lee, S.; Park, C.; Choi, Y.; Kim, C. Effect of ignition timing retard strategy on NOx reduction in hydrogen-compressed natural gas blend engine with increased compression ratio. *Int. J. Hydrogen Energy* **2014**, *39*, 2399–2408. [CrossRef]
2. Pastor, J.V.; García-Oliver, J.M.; García, A.; Pinotti, M. Effect of laser induced plasma ignition timing and location on Diesel spray combustion. *Energy Convers. Manag.* **2017**, *133*, 41–55. [CrossRef]
3. Şöhret, Y.; Gürbüz, H.; Akçay, İ.H. Energy and exergy analyses of a hydrogen fueled SI engine: Effect of ignition timing and compression ratio. *Energy* **2019**, *175*, 410–422. [CrossRef]
4. Saravanan, S.; Nagarajan, G.; Rao, G.L.N.; Sampath, S. Theoretical and experimental investigation on effect of injection timing on NOx emission of biodiesel blend. *Energy* **2014**, *66*, 216–221. [CrossRef]
5. Agarwal, A.K.; Dhar, A.; Gupta, J.G.; Kim, W.I.; Lee, C.S.; Park, S. Effect of fuel injection pressure and injection timing on spray characteristics and particulate size-number distribution in a biodiesel fuelled common rail direct injection diesel engine. *Appl. Energy* **2014**, *130*, 212–221. [CrossRef]
6. Aljamali, S.; Abdullah, S.; Mahmood, W.M.F.W.; Ali, Y. Effect of fuel injection timings on performance and emissions of stratified combustion CNGDI engine. *Appl. Therm. Eng.* **2016**, *109*, 619–629. [CrossRef]
7. Verhelst, S.; Turner, J.W.; Sileghem, L.; Vancoillie, J. Methanol as a fuel for internal combustion engines. *Prog. Energy Combust. Sci.* **2019**, *70*, 43–88. [CrossRef]
8. Tartakovsky, L.; Sheintuch, M. Fuel reforming in internal combustion engines. *Prog. Energy Combust. Sci.* **2018**, *67*, 88–114. [CrossRef]

9. Lee, J.; Park, C.; Kim, Y.; Choi, Y.; Bae, J.; Lim, B. Effect of turbocharger on performance and thermal efficiency of hydrogen-fueled spark ignition engine. *Int. J. Hydrogen Energy* **2019**, *44*, 4350–4360. [CrossRef]
10. Verhelst, S.; Maesschalck, P.; Rombaut, N.; Sierens, R. Increasing the power output of hydrogen internal combustion engines by means of supercharging and exhaust gas recirculation. *Int. J. Hydrogen Energy* **2009**, *34*, 4406–4412. [CrossRef]
11. Rajput, R.K. *Text Book "Internal Combusion Engine"*; Laxmi-Publications: Delhi, India, 2008. Available online: https://www.kopykitab.com/A-Textbook-Of-Internal-Combustion-Engines-by-Er-R-K-Rajput (accessed on 15 January 2021).
12. Ganesan, V. *Text Book "Internal Combustion Engine"*; Tata McGraw-Hill: New York, NY, USA, 2012. Available online: https://books.google.com.vn/books?id=hfejAwAAQBAJ&printsec=frontcover&dq=internal+combustion+engine+book&hl=vi&sa=X&redir_esc=y#v=onepage&q=internal%20combustion%20engine%20book&f=false (accessed on 15 January 2021).
13. Ayhan, V.; Ece, Y.M. New application to reduce NOx emissions of diesel engines: Electronically controlled direct water injection at compression stroke. *Appl. Energy* **2020**, *260*, 114328. [CrossRef]
14. Li, A.; Zheng, Z.; Peng, T. Effect of water injection on the knock, combustion, and emissions of a direct injection gasoline engine. *Fuel* **2020**, *268*, 117376. [CrossRef]
15. Xu, P.; Ji, C.; Wang, S.; Cong, X.; Ma, Z.; Tang, C.; Meng, H.; Shi, C. Effects of direct water injection on engine performance in engine fueled with hydrogen at varied excess air ratios and spark timing. *Fuel* **2020**, *269*, 117209. [CrossRef]
16. Zhuang, Y.; Sun, Y.; Huang, Y.; Teng, Q.; He, B.; Chen, W.; Qian, Y. Investigation of water injection benefits on downsized boosted direct injection spark ignition engine. *Fuel* **2020**, *264*, 116765. [CrossRef]
17. Zhu, S.; Hu, B.; Akehurst, S.; Copeland, C.; Lewis, A.; Yuan, H.; Kennedy, I.; Bernards, J.; Branney, C. A review of water injection applied on the internal combustion engine. *Energy Convers. Manag.* **2018**, *184*, 139–158. [CrossRef]
18. Xu, J.; Chen, G.; Guo, F.; Xie, J. Development of wide-temperature vanadium-based catalysts for selective catalytic reducing of NOx with ammonia: Review. *Chem. Eng. J.* **2018**, *353*, 507–518. [CrossRef]
19. Mohan, S.; Dinesha, P.; Kumar, S. NOx reduction behaviour in copper zeolite catalysts for ammonia SCR systems: A review. *Chem. Eng. J.* **2020**, *384*, 123253. [CrossRef]
20. Ye, B.; Lee, M.; Jeong, B.; Kim, J.; Lee, D.H.; Baik, J.M.; Kim, H.D. Partially reduced graphene oxide as a support of Mn-Ce/TiO_2 catalyst for selective catalytic reduction of NOx with NH_3. *Catal. Today* **2018**, *328*, 300–306. [CrossRef]
21. Pan, M.; Zheng, Z.; Huang, R.; Zhou, X.; Huang, H.; Pan, J.; Chen, Z. Reduction in PM and NOX of a diesel engine integrated with n-octanol fuel addition and exhaust gas recirculation. *Energy* **2019**, *187*, 115946. [CrossRef]
22. Park, H.; Shim, E.; Bae, C. Improvement of combustion and emissions with exhaust gas recirculation in a natural gas-diesel dual-fuel premixed charge compression ignition engine at low load operations. *Fuel* **2018**, *235*, 763–774. [CrossRef]
23. Pratheeba, C.N.; Aghalayam, P. Effect of Exhaust Gas Recirculation in NOx Control for Compression Ignition and Homogeneous Charge Compression Ignition Engines. *Phys. Procedia* **2015**, *66*, 25–28. [CrossRef]
24. Heffel, J.W. NOx emission and performance data for a hydrogen fueled internal combustion engine at 1500 rpm using exhaust gas recirculation. *Int. J. Hydrogen Energy* **2003**, *28*, 901–908. [CrossRef]
25. Asad, U.; Zheng, M. Exhaust gas recirculation for advanced diesel combustion cycles. *Appl. Energy* **2014**, *123*, 242–252. [CrossRef]
26. Venu, H.; Subramani, L.; Raju, V.D. Emission reduction in a DI diesel engine using exhaust gas recirculation (EGR) of palm biodiesel blended with TiO_2 nano additives. *Renew. Energy* **2019**, *140*, 245–263. [CrossRef]
27. Gonzalez, M.A.D.; di Nunno, D. Internal Exhaust Gas Recirculation for Efficiency and Emissions in a 4-Cylinder Diesel Engine. In Proceedings of the SAE 2016 International Powertrains, Fuels & Lubricants Meeting, Baltimore, MD, USA, 24–26 October 2016. [CrossRef]
28. Shi, L.; Cui, Y.; Deng, K.; Peng, H.; Chen, Y. Study of low emission homogeneous charge compression ignition (HCCI) engine using combined internal and external exhaust gas recirculation (EGR). *Energy* **2006**, *31*, 2665–2676. [CrossRef]
29. Jimbo, T.; Hayakawa, Y. Model predictive control for automotive engine torque considering internal exhaust gas recirculation. *IFAC Proc. Vol.* **2011**, *44*, 12991–12997. [CrossRef]
30. Guardiola, C.; Triantopoulos, V.; Bares, P.; Bohac, S.; Stefanopoulou, A. Simultaneous Estimation of Intake and Residual Mass Using In-Cylinder Pressure in an Engine with Negative Valve Overlap. *IFAC-PapersOnLine* **2016**, *49*, 461–468. [CrossRef]
31. Zhao, H. Four-stroke CAI engines with residual gas trapping. *HCCI CAI Engines Automot. Ind.* **2007**, 103–135. [CrossRef]
32. Verschaeren, R.; Schaepdryver, W.; Serruys, T.; Bastiaen, M.; Vervaeke, L.; Verhelst, S. Experimental study of NOx reduction on a medium speed heavy duty diesel engine by the application of EGR (exhaust gas recirculation) and Miller timing. *Energy* **2014**, *76*, 614–621. [CrossRef]
33. Liu, L.; Li, Z.; Liu, S.; Shen, B. Effect of exhaust gases of Exhaust Gas Recirculation (EGR) coupling lean-burn gasoline engine on NOx purification of Lean NOx trap (LNT). *Mech. Syst. Signal Process.* **2017**, *87*, 195–213. [CrossRef]
34. Fu, J.; Zhu, G.; Zhou, F.; Liu, J.; Xia, Y.; Wang, S. Experimental investigation on the influences of exhaust gas recirculation coupling with intake tumble on gasoline engine economy and emission performance. *Energy Convers. Manag.* **2016**, *127*, 424–436. [CrossRef]
35. Sher, E. *Handbook of Air Pollution From Internal Combustion Engines*; Academic Press: Cambridge, MA, USA, 1998.
36. Abd-Alla, G.H. Using exhaust gas recirculation in internal combustion engines: A review. *Energy Convers. Manag.* **2002**, *43*, 1027–1042. [CrossRef]
37. Zheng, M.; Reader, G.T.; Hawley, J.G. Diesel engine exhaust gas recirculation—A review on advanced and novel concepts. *Energy Convers. Manag.* **2004**, *45*, 883–900. [CrossRef]

38. Sorathia, H.S.; Rahhod, P.P.; Sorathiya, A.S.; Engineering, M.; College, G.E.; Kutch, B. Effect of Exhaust Gas Recirculation (EGR) on NOx emission CI engine—A review study. *Ijaers* **2012**, *1*, 223–227.
39. Thangaraja, J.; Kannan, C. Effect of exhaust gas recirculation on advanced diesel combustion and alternate fuels—A review. *Appl. Energy* **2016**, *180*, 169–184. [CrossRef]
40. Verma, S.; Das, L.M.; Kaushik, S.C.; Bhatti, S.S. The effects of compression ratio and EGR on the performance and emission characteristics of diesel-biogas dual fuel engine. *Appl. Therm. Eng.* **2018**, *150*, 1090–1103. [CrossRef]
41. Kavuri, C.; Kokjohn, S.L. Computational optimization of a reactivity controlled compression ignition (RCCI) combustion system considering performance at multiple modes simultaneously. *Fuel* **2017**, *207*, 702–718. [CrossRef]
42. Burtscher, H. Physical characterization of particulate emissions from diesel engines: A review. *J. Aerosol Sci.* **2005**, *36*, 896–932. [CrossRef]
43. Xu, G.; Jia, M.; Li, Y.; Chang, Y.; Liu, H.; Wang, T. Evaluation of variable compression ratio (VCR)and variable valve timing (VVT)strategies in a heavy-duty diesel engine with reactivity controlled compression ignition (RCCI)combustion under a wide load range. *Fuel* **2019**, *253*, 114–128. [CrossRef]
44. Hirkude, J.; Belokar, V.; Randhir, J. Effect of Compression Ratio, Injection Pressure and Injection Timing on Performance and Smoke Emissions of CI engine Fuelled with Waste Fried Oil Methyl Esters—Diesel Blend. *Mater. Today Proc.* **2018**, *5*, 1563–1570. [CrossRef]
45. Kirchstetter, T.W.; Harley, R.A.; Kreisberg, N.M.; Stolzenburg, M.R.; Hering, S.V. On-road measurement of fine particle and nitrogen oxide emissions from light- and heavy-duty motor vehicles. *Atmos. Environ.* **1999**, *33*, 2955–2968. [CrossRef]
46. Torregrosa, A.J.; Broatch, A.; Olmeda, P.; Salvador-Iborra, J.; Warey, A. Experimental study of the influence of exhaust gas recirculation on heat transfer in the firedeck of a direct injection diesel engine. *Energy Convers. Manag.* **2017**, *153*, 304–312. [CrossRef]
47. Agarwal, D.; Singh, S.K.; Agarwal, A.K. Effect of Exhaust Gas Recirculation (EGR) on performance, emissions, deposits and durability of a constant speed compression ignition engine. *Appl. Energy* **2011**, *88*, 2900–2907. [CrossRef]
48. Dennis, A.J.; Garner, C.P.; Taylor, D.H.C. The Effect of EGR on Diesel Engine Wear. SAE International: Warrendale, PA, USA, 1999.
49. George, S.; Balla, S.; Gautam, M. Effect of diesel soot contaminated oil on engine wear. *Wear* **2006**, *262*, 1113–1122. [CrossRef]
50. Wang, D.; Shi, L.; Zhu, S.; Liu, B.; Qian, Y.; Deng, K. Numerical and thermodynamic study on effects of high and low pressure exhaust gas recirculation on turbocharged marine low-speed engine. *Appl. Energy* **2020**, *261*, 114346. [CrossRef]
51. Awad, O.I.; Mamat, R.; Ali, O.M.; Sidik, N.A.C.; Yusaf, T.; Kadirgama, K.; Kettner, M. Alcohol and ether as alternative fuels in spark ignition engine: A review. *Renew. Sustain. Energy Rev.* **2017**, *82*, 2586–2605. [CrossRef]
52. Mamat, R.; Sani, M.S.M.; Sudhakar, K.; Kadarohman, A.; Sardjono, R.E. An overview of Higher alcohol and biodiesel as alternative fuels in engines. *Energy Rep.* **2019**, *5*, 467–479. [CrossRef]
53. Balki, M.K.; Sayin, C. The effect of compression ratio on the performance, emissions and combustion of an SI (spark ignition) engine fueled with pure ethanol, methanol and unleaded gasoline. *Energy* **2014**, *71*, 194–201. [CrossRef]
54. Rosha, P.; Mohapatra, S.K.; Mahla, S.K.; Cho, H.M.; Chauhan, B.S.; Dhir, A. Effect of compression ratio on combustion, performance, and emission characteristics of compression ignition engine fueled with palm (B20)biodiesel blend. *Energy* **2019**, *178*, 676–684. [CrossRef]
55. Lee, J.; Park, C.; Bae, J.; Kim, Y.; Choi, Y.; Lim, B. Effect of different excess air ratio values and spark advance timing on combustion and emission characteristics of hydrogen-fueled spark ignition engine. *Int. J. Hydrogen Energy* **2019**, *44*, 25021–25030. [CrossRef]
56. Lata, D.B.; Misra, A.; Medhekar, S. Investigations on the combustion parameters of a dual fuel diesel engine with hydrogen and LPG as secondary fuels. *Int. J. Hydrogen Energy* **2011**, *36*, 13808–13819. [CrossRef]
57. Shukla, P.C.; Belgiorno, G.; di Blasio, G.; Agarwal, A.K. *Alcohol as an Alternative Fuel for Internal Combustion Engines*; Springer: Berlin/Heidelberg, Germany, 2021.
58. Li, Y.; Jia, M.; Chang, Y.; Fan, W.; Xie, M.; Wang, T. Evaluation of the necessity of exhaust gas recirculation employment for a methanol/diesel reactivity controlled compression ignition engine operated at medium loads. *Energy Convers. Manag.* **2015**, *101*, 40–51. [CrossRef]
59. Saravanan, P.; Kumar, N.M.; Ettappan, M.; Dhanagopal, R.; Vishnupriyan, J. Effect of exhaust gas re-circulation on performance, emission and combustion characteristics of ethanol-fueled diesel engine. *Case Stud. Therm. Eng.* **2020**, *20*, 100643. [CrossRef]
60. Sun, C.; Liu, Y.; Qiao, X.; Ju, D.; Tang, Q.; Fang, X.; Zhou, F. Experimental study of effects of exhaust gas recirculation on combustion, performance, and emissions of DME-biodiesel fueled engine. *Energy* **2020**, *197*, 117233. [CrossRef]
61. Zhao, Y.; Wang, Y.; Li, D.; Lei, X.; Liu, S. Combustion and emission characteristics of a DME (dimethyl ether)-diesel dual fuel premixed charge compression ignition engine with EGR (exhaust gas recirculation). *Energy* **2014**, *72*, 608–617. [CrossRef]
62. Salvi, B.L.; Subramanian, K.A. Experimental investigation on effects of compression ratio and exhaust gas recirculation on backfire, performance and emission characteristics in a hydrogen fuelled spark ignition engine. *Int. J. Hydrogen Energy* **2016**, *41*, 5842–5855. [CrossRef]
63. Salvi, B.L.; Subramanian, K.A. Experimental investigation on effects of exhaust gas recirculation on flame kernel growth rate in a hydrogen fuelled spark ignition engine. *Appl. Therm. Eng.* **2016**, *107*, 48–54. [CrossRef]
64. Das, L.M.; Mathur, R. Exhaust gas recirculation for Nox control in a multicylinder hydrogen-supplemented S.I. engine. *Int. J. Hydrogen Energy* **1993**, *18*, 1013–1018. [CrossRef]

65. Yasin, M.H.M.; Mamat, R.; Yusop, A.F.; Paruka, P.; Yusaf, T.; Najafi, G. Effects of Exhaust Gas Recirculation (EGR) on a Diesel Engine fuelled with Palm-biodiesel. *Energy Procedia* **2015**, *75*, 30–36. [CrossRef]
66. Jung, D.; Lee, S. An investigation on the potential of dedicated exhaust gas recirculation for improving thermal efficiency of stoichiometric and lean spark ignition engine operation. *Appl. Energy* **2018**, *228*, 1754–1766. [CrossRef]
67. Bozza, F.; de Bellis, V.; Teodosio, L. Potentials of cooled EGR and water injection for knock resistance and fuel consumption improvements of gasoline engines. *Appl. Energy* **2016**, *169*, 112–125. [CrossRef]
68. Lee, S.; Park, S.; Kim, C.; Kim, Y.M.; Kim, Y.; Park, C. Comparative study on EGR and lean burn strategies employed in an SI engine fueled by low calorific gas. *Appl. Energy* **2014**, *129*, 10–16. [CrossRef]
69. Lattimore, T.; Wang, C.; Xu, H.; Wyszynski, M.L.; Shuai, S. Investigation of EGR Effect on Combustion and PM Emissions in a DISI Engine. *Appl. Energy* **2016**, *161*, 256–267. [CrossRef]
70. Takaki, D.; Tsuchida, H.; Kobara, T.; Akagi, M.; Tsuyuki, T.; Nagamine, M. Study of an egr system for downsizing turbocharged gasoline engine to improve fuel economy. *SAE Tech. Pap.* **2014**, *1*, 1–8. [CrossRef]
71. Lean-burn, C.B. Comparison Between Lean-Burn and Stoichiometric Technologies for CNG Heavy-Duty Engines. In *SAE Transactions*; SAE International: Warrendale, PA, USA, 1995; pp. 20–22.
72. Gupta, A.; Abdel-Gayed, R. Qualitative Governing Approach of a Spark Ignition Engine Using Exhaust Gas Recirculation. *Phys. Procedia* **2015**, *66*, 97–100. [CrossRef]
73. Cai, L.; Ramalingam, A.; Minwegen, H.; Heufer, K.A.; Pitsch, H. Impact of exhaust gas recirculation on ignition delay times of gasoline fuel: An experimental and modeling study. *Proc. Combust. Inst.* **2019**, *37*, 639–647. [CrossRef]
74. Wei, H.; Zhu, T.; Shu, G.; Tan, L.; Wang, Y. Gasoline engine exhaust gas recirculation—A review. *Appl. Energy* **2012**, *99*, 534–544. [CrossRef]
75. Ladommatos, N.; Abdelhalim, S.M.; Zhao, H.; Hu, Z. The dilution, chemical, and thermal effects of exhaust gas recirculation on diesel engine emissions-part 2: Effects of carbon dioxide. *SAE Trans.* **1996**, 1844–1862. [CrossRef]
76. Kohketsu, S.; Mori, K.; Sakai, K.; Hakozaki, T. EGR technologies for a turbocharged and intercooled heavy-duty diesel engine. *SAE Trans.* **1997**, 482–489. [CrossRef]
77. Baert, R.S.G.; Beckman, D.E.; Veen, A. Efficient EGR technology for future HD diesel engine emission targets. *SAE Trans.* **1999**, 381–393. [CrossRef]
78. Lehto, K.; Elonheimo, A.; Häkkinen, K.; Sarjovaara, T.; Larmi, M. Emission reduction using hydrotreated vegetable oil (HVO) with miller timing and EGR in diesel combustion. *SAE Int. J. Fuels Lubr.* **2011**, *5*, 218–224. [CrossRef]
79. Andwari, A.M.; Aziz, A.A.; Said, M.F.M.; Latiff, Z.A. Experimental investigation of the influence of internal and external EGR on the combustion characteristics of a wcontrolled auto-ignition two-stroke cycle engine. *Appl. Energy* **2014**, *134*, 1–10. [CrossRef]
80. Baratta, M.; Finesso, R.; Misul, D.; Spessa, E. Comparison between Internal and External EGR Performance on a Heavy Duty Diesel Engine by Means of a Refined 1D Fluid-Dynamic Engine Model. *SAE Int. J. Engines* **2015**, *8*, 1977–1992. [CrossRef]
81. Kozarac, D.; Vuilleumier, D.; Saxena, S.; Dibble, R.W. Analysis of benefits of using internal exhaust gas recirculation in biogas-fueled HCCI engines. *Energy Convers. Manag.* **2014**, *87*, 1186–1194. [CrossRef]
82. Szwaja, S.; Ansari, E.; Rao, S.; Szwaja, M.; Grab-Rogalinski, K.; Naber, J.D.; Pyrc, M. Influence of exhaust residuals on combustion phases, exhaust toxic emission and fuel consumption from a natural gas fueled spark-ignition engine. *Energy Convers. Manag.* **2018**, *165*, 440–446. [CrossRef]
83. da Costa RB, R.; Hernández, J.J.; Teixeira, A.F.; Netto NA, D.; Valle, R.M.; Roso, V.R.; Coronado, C.J. Combustion, performance and emission analysis of a natural gas-hydrous ethanol dual-fuel spark ignition engine with internal exhaust gas recirculation. *Energy Convers. Manag.* **2019**, *195*, 1187–1198. [CrossRef]
84. Zhou, L.; Hua, J.; Liu, F.; Liu, F.; Feng, D.; Wei, H. Effect of internal exhaust gas recirculation on the combustion characteristics of gasoline compression ignition engine under low to idle conditions. *Energy* **2018**, *164*, 306–315. [CrossRef]
85. Khoa, N.X.; Lim, O. Comparative Study of the Effective Release Energy, Residual Gas Fraction, and Emission Characteristics with Various Valve Port Diameter-Bore Ratios (VPD/B) of a Four-Stroke Spark Ignition Engine. *Energies* **2020**, *13*, 1330. [CrossRef]
86. Khoa, N.X.; Kang, Y.; Lim, O. The effects of combustion duration on residual gas, effective release energy and engine power of motorcycle engine at full load. *Energy Procedia* **2019**, *158*, 1835–1841. [CrossRef]
87. Khoa, N.X.; Lim, O. The effects of combustion duration on residual gas, effective release energy, engine power and engine emissions characteristics of the motorcycle engine. *Appl. Energy* **2019**, *248*, 54–63. [CrossRef]
88. Khoa, N.X.; Nhu, Y.Q.; Lim, O. Estimation of parameters affected in internal exhaust residual gases recirculation and the influence of exhaust residual gas on performance and emission of a spark ignition engine. *Appl. Energy* **2020**, *278*, 115699. [CrossRef]
89. Albert, B.P. Residual Gas Effects on Combustion in an Air-Cooled Utility Engine. Master's Thesis, University of Wisconsin-Madison, Madison, WI, USA, 2004.
90. Khoa, N.X.; Lim, O.T. Effective release energy, residual gas, and engine emission characteristics of a V-twin engine with various exhaust valve closing timings. *J. Mech. Sci. Technol.* **2020**, *34*, 477–488. [CrossRef]
91. Turner, J.W.G.; Bassett, M.D.; Pearson, R.J.; Pitcher, G.; Douglas, K.J. New operating strategies afforded by fully variable valve trains. In *2004 SAE World Congress*; SAE International: Warrendale, PA, USA, 2004.
92. Milovanovic, N.; Dave, B.; Gedge, S.; Turner, J. Cam Profile Switching (CPS) and phasing strategy vs Fully Variable Valve Train (FVVT) strategy for transitions between spark ignition and controlled auto ignition modes. In *2005 SAE World Congress*; SAE International: Warrendale, PA, USA, 2005; Volume 724. [CrossRef]

93. Shao, D.; Sichuan, X.; Du, A. Research on a New Electromagnetic Valve Actuator Based on Voice Coil Motor for Automobile Engines. In *SAE Technical Paper*; SAE International: Warrendale, PA, USA, 2017. [CrossRef]
94. Schwoerer, J.; Dodi, S.; Fox, M.; Huang, S.; Yang, Z. Internal EGR systems for NOx emission reduction in heavy-duty diesel engines. In *SAE Technical Paper*; SAE International: Warrendale, PA, USA, 2004; Volume 724. [CrossRef]
95. Millo, F.; Mallamo, F.; Arnone, L.; Bonanni, M.; Franceschini, D. Analysis of different internal EGR solutions for small diesel engines. In *SAE Technical Paper*; SAE International: Warrendale, PA, USA, 2007; Volume 724. [CrossRef]
96. Benajes, J.; Reyes, E.; Luján, J.M. Intake valve pre-lift effect on the performance of a turbocharged diesel engine. In *SAE Technical Paper*; SAE International: Warrendale, PA, USA, 1996; Volume 96, pp. 1407–1476. [CrossRef]
97. Knecht, W. Potential of Variable Valve Actuation in Diesel Engines for Light Duty Vehicles. In Proceedings of the ATA International Symposium on the Future of Diesel Engine Technology for Passenger Cars, Costa Smerelda, Italy, 12–13 October 2000.
98. Vafidis, C.; Piccinini, A.; Gianolio, L. Variable Valve Actuation for In-Cylinder Charge and Combustion Control in D.I. Diesel Engines. In Proceedings of the IFP International Congress a New Generation of Engine Combustion Processes for the Future, Rueil Malmaison, France, 26–27 November 2001.
99. Lanzanova, T.D.M.; Nora, M.D.; Martins, M.E.S.; Machado, P.R.M.; Pedrozo, V.B.; Zhao, H. The effects of residual gas trapping on part load performance and emissions of a spark ignition direct injection engine fuelled with wet ethanol. *Appl. Energy* **2019**, *253*, 113508. [CrossRef]
100. Cho, G.; Moon, G.; Jeong, D.; Bae, C. Effects of internal exhaust gas recirculation on controlled auto-ignition in a methane engine combustion. *Fuel* **2009**, *88*, 1042–1048. [CrossRef]
101. Duan, X.; Liu, Y.; Liu, J.; Lai, M.C.; Jansons, M.; Guo, G.; Zhang, S.; Tang, Q. Experimental and numerical investigation of the effects of low-pressure, high-pressure and internal EGR configurations on the performance, combustion and emission characteristics in a hydrogen-enriched heavy-duty lean-burn natural gas SI engine. *Energy Convers. Manag.* **2019**, *195*, 1319–1333. [CrossRef]